

Contents lists available at ScienceDirect

Nano Materials Science

journal homepage: www.keaipublishing.com/cn/journals/nano-materials-science/

Geometric structures, electronic characteristics, stabilities, catalytic activities, and descriptors of graphene-based single-atom catalysts



Weijie Yang^a, Shaopeng Xu^a, Kai Ma^a, Chongchong Wu^b, Ian D. Gates^{b,**}, Xunlei Ding^c, Weihua Meng^{d,***}, Zhengyang Gao^{a,*}

^a School of Energy and Power Engineering, North China Electric Power University, Baoding, 071003, China

^b Department of Chemical and Petroleum Engineering, University of Calgary, T2N 1N4, Calgary, Alberta, Canada

^c School of Mathematics and Physics, North China Electric Power University, Beijing, 102206, China

^d The Flame Retardant Material and Processing Technology Engineering Research Center of Hebei Province, College of Chemistry and Environmental Science, Hebei University, Baoding, 071002, China

ARTICLE INFO

Keywords:

Single-atom catalyst
Graphene
Stability
Activity
Density functional theory
Reaction descriptor

ABSTRACT

Single-atom catalysts (SACs) have been a research hotspot due to their high catalytic activity, selectivity, and atomic utilization rates. However, the theoretical research of SACs is relatively fragmented, which restricts further understanding of SAC stability and activity. To address this issue, we report our analysis of the geometric structures, electronic characteristics, stabilities, catalytic activities, and descriptors of 132 graphene-based single-atom catalysts (M/GS) obtained from density functional theory calculations. Based on the calculated formation and binding energies, a stability map of M/GS was established to guide catalyst synthesis. The effects of metal atoms and support on the charge of metal atoms are discussed. The catalytic activities of M/GS in both nitrogen and oxygen reduction reactions are predicted based on the calculated magnetic moment and the adsorption energy. Combined with the electronegativity and *d*-band center, a two-dimensional descriptor is proposed to predict the O adsorption energy on M/GS. More importantly, this theoretical study provides predictive guidance for the preparation and rational design of highly stable and active single-atom catalysts using nitrogen doping on graphene.

1. Introduction

Recently, single-atom catalysts (SACs) have been a focal point in energy and chemical engineering due to their high catalytic activity, selectivity and atomic utilization rate [1,2]. Preparations of various SACs have been reported, such as Pt₁/FeO_x [3], Rh₁/CoO [4], Pd₁/Fe₂O₃ [5], and M-N₄-C (M = Fe, Co, and Ni) [6–9]. Due to the large specific surface area and unique physicochemical properties of graphene, SACs supported with graphene-based substrates (M/GS) have been widely applied in catalysis including CO oxidation [10–15], CO₂ reduction [16–18], water splitting [19,20], and oxidation-reduction reaction [8,21–23]. Due to their importance in catalytic reactions, the stability and catalytic activity of SACs have become key issues in the evaluation of M/GS [1, 24–26].

Although various M/GS can successfully be prepared experimentally

through high temperature calcination and chemical leaching processes [27–30], ensuring high stability during processing is still challenging, especially for high-loading M/GS. The stability of SACs has been a critical issue due to their tendency to agglomerate into clusters or nanoparticles [1,24]. To investigate the agglomeration of single atoms, the binding energy of the metal dopant on graphene-based substrates has been studied using density functional theory (DFT) calculations in previous studies [31–35]. Wang et al. [20] compared the binding energy of metal atoms with the corresponding cohesive energy and concluded that the adsorption of Ba, Mg, and Ti on the graphene-based substrate is strong enough to prevent the agglomeration of metal atoms. However, some previous studies only focused on the binding energy, and neglected the cohesive energy of metallic bulk. Liu et al. [36] calculated the binding energy of Pd on N-doped single vacancy graphene-based substrate (−3.02 eV) and concluded that the graphene-based substrate could bind

* Corresponding author.

** Corresponding author.

*** Corresponding author.

E-mail addresses: idgates@ucalgary.ca (I.D. Gates), mengweihua121@163.com (W. Meng), gaozhyang@163.com (Z. Gao).

<https://doi.org/10.1016/j.nanoms.2019.10.008>

Received 27 September 2019; Accepted 22 October 2019

Available online 6 November 2019

2589-9651/© 2020 Chongqing University. Production and hosting by Elsevier B.V. on behalf of KeAi. This is an open access article under the CC BY-NC-ND license

(<http://creativecommons.org/licenses/by-nc-nd/4.0/>).

the Pd atom strongly, thus having good catalytic stability. However, this binding energy (-3.02 eV) is weaker than the cohesive energy of bulk Pd (-3.90 eV) [37], suggesting that Pd atoms are likely to agglomerate and subsequently form nanoparticles. Also, the binding energy of Pt on a single vacancy graphene-based substrate is -4.47 eV [32], which is weaker than the cohesive energy of bulk Pt (-5.85 eV) [37].

Based on the above discussion, the current research based on the binding energy versus the cohesive energy is insufficient to accurately evaluate the tendency of metal atoms to agglomerate.

On the other hand, formation energy determines the thermodynamic stability of catalysts [38–40], which provides an important guide for catalyst synthesis. However, there is still a lack of consideration of the formation energy in previous theoretical studies of M/GS [41]. In addition, there are currently two different calculation formulas for formation energy of M/GS. Some studies consider the formation energy of graphene-based substrates [20,38,42], while others neglect the contribution of graphene-based substrates on the formation energy [39,40]. Considering that the formation energies of M/GS can be calculated by different formulas, this leads to a lack of comparability of the formation energy data in the literature. Therefore, it is necessary to study formation energy systematically using a uniform calculation formula.

Regarding the catalytic activity of M/GS, there have been a large number of theoretical studies focused on SACs, which typically investigated a given specific reaction using different computation methods [20–24]. However, a simple descriptor that correlates catalytic structure and activity has not been developed, which limits the effective screening of catalysts. To describe the potential energy variations in catalytic reactions [43], scaling relationships [44] and Brønsted-Evans-Polanyi (BEP) correlations [45] have been proposed; these have been applied in many catalytic reactions [46–48]. Combined with the scaling and BEP relationships, the energy barrier of catalytic reactions and the activity of catalysts can be predicted solely based on the adsorption energy of a small adsorbate [49,50]. To bridge the gap between catalyst structure and adsorption energy, the d -band center (ϵ_d) theory proposed by Nørskov et al. [51] has been successfully applied in the evaluation of CO [51], and CO₂ adsorption [52]. However, the prediction of ϵ_d on the adsorption energy of H, O, OH, and OOH has been proved to be less effective [53–57]. In addition, ϵ_d has been proved to be an inappropriate descriptor of adsorption energy for SAC systems [58–60]. Therefore, to facilitate catalyst screening, it is necessary to develop a simple and effective descriptor of adsorption energy in M/GS systems.

According to the research mentioned above, the investigation of catalyst stability based on binding energy and formation energy in the system of M/GS is scattered, and an effective descriptor of adsorption energy is lacking, thus hindering the development of highly stable and active M/GS. Therefore, it is imperative to perform a systematic theoretical study of the geometric structures, electronic characteristics, stabilities, catalytic activities, and descriptors of graphene-based SACs in order to prepare and design highly stable and active M/GS.

In this research, we studied 12 metal atoms and 11 graphene-based substrates, for a total of 132 M/GS systems. First, the geometric structures of M/GS including bond length and elevation height were evaluated. Second, the charge of the metal atom and d -band center, as key parameters, were calculated to study the electronic characteristics. Third, to guide the synthesis of catalysts, a stability map of M/GS was established based on the formation and binding energies of M/GS. Subsequently, the catalytic activities of M/GS in a nitrogen reduction reaction (NRR) and oxygen reduction reaction (ORR) were predicted, respectively, based on the calculated magnetic moment and the oxygen adsorption energy. Finally, combined with the electronegativity and d -band center, an effective activity descriptor of M/GS is proposed to predict the adsorption energy of oxygen on the surface of M/GSs.

2. Methods

2.1. Computation methods

All DFT calculations were conducted using the Vienna *ab initio* simulation package (VASP) using the Perdew-Burke-Ernzerhof (PBE) functional and projector augmented wave (PAW) methods [61–63]. The combination of PBE and PAW methods has been adopted for the calculation of adsorption and catalytic reaction on M/GS [4,38–40,60,64–70]. To determine the magnetic properties of the system, spin-polarization was employed to acquire the accurate ground-state energy [71]. Consistent with our previous model [33,69], a (4×4) supercell of graphene with a 15 \AA vacuum layer was adopted as the model's graphene-based substrate.

The kinetic energy cutoff of the plane-wave basis set was set as 500 eV. Gaussian smearing ($\sigma = 0.05$ eV) was adopted for the occupation of the electronic levels. A $(7 \times 7 \times 1)$ Γ -centered k -point grid was selected for structural relaxations, which has been shown to be accurate in our previous studies [33,69]. Specifically, a convergent structure optimization was defined as occurring when all the forces fell below 0.02 eV/Å. To acquire a more accurate electronic structure, a $(15 \times 15 \times 1)$ Γ -centered k -point grid was adopted for the energy calculations to determine both the system energy and the charge information.

M/GS are usually synthesized through physical [8,9,22,72] and chemical [6,73] methods by using graphene [9,22] or graphene oxide [8,17,73] as the raw materials. Therefore, the formation process of M/GS should start with graphene, and the formation energy of defective and doped graphene-based substrates should be included in the formation energy calculations of M/GS. The formation energy of the substrates and the M/GS can be calculated using the following equations (1) [34] and (2) [38], respectively:

$$\text{for the substrate: } E_f = E_{\text{Sub}} + x\mu_C - E_G - y\mu_N, \text{ or} \quad (1)$$

$$\text{for the M/GS: } E_f = E_{\text{M/GS}} + x\mu_C - E_G - y\mu_N - E_M, \quad (2)$$

where E_{Sub} is the total energy of the graphene-based substrate; x is the number of carbon atoms removed from the pristine graphene; μ_C is the chemical potential of carbon defined as the total energy per carbon atom for pristine graphene; y is the number of nitrogen atoms added; μ_N is the chemical potential of nitrogen (defined as half of the total energy of an N₂ molecule); E_M is the total energy of an isolated metal atom in the vacuum; and $E_{\text{M/GS}}$ is the total energy of M/GS. According to this definition, a negative E_f value indicates a thermodynamically favorable configuration, whereas a more negative value of E_f corresponds to a higher thermodynamic stability. The binding energy of metal atoms on substrates can be calculated according to the formula:

$$E_b = E_{\text{M/GS}} - E_{\text{Sub}} - E_M. \quad (3)$$

The adsorption energy of oxygen on M/GS is defined by:

$$E_{\text{ads}}(\text{O}) = E_{\text{tot}} - E_{\text{M/GS}} - E_{\text{O}}, \quad (4)$$

where E_{tot} is the total energy of the adsorption system of oxygen; and E_{O} is the energy of oxygen, which is half of the energy of an oxygen molecule. The d -band center of the catalyst can be calculated from Ref. [51]:

$$\epsilon_d = \frac{\int_{-\infty}^{+\infty} E \cdot D(E) dE}{\int_{-\infty}^{+\infty} D(E) dE}, \quad (5)$$

where $D(E)$ is the total d states of the metal atom in M/GS.

2.2. Modeling

There are two types of M/GS according to the number of vacancy defects in graphene-based substrates. In Fig. 1, structures (a-d) belong to

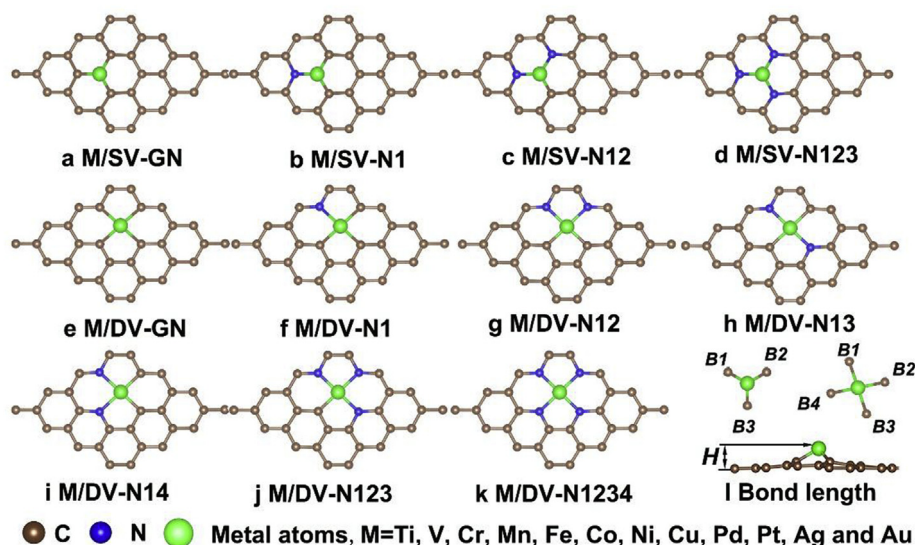


Fig. 1. Structures of SACs with different graphene-based substrates.

SACs with single vacancy substrates (M/SV-GS), while structures (e-k) belong to those SACs with double vacancies substrates (M/DV-GS). Taking into account the catalyst synthesis, both vacancy defects and the doping of nitrogen are common and accessible modification methods. Therefore, 11 types of graphene-based substrates were selected to study the support effects on catalytic performance. In detail, three nonequivalent structures in two nitrogen atoms were embedded into the graphene-based substrates according to the different coordination environments of the metal atoms. These structures were labeled as M/DV-N12, M/DV-N13, and M/DV-N14, respectively. Fig. 1 shows that there are three bonds adjacent to metal atoms in M/SV-GS (denoted as B1, B2, and B3), and there are four bonds adjacent to metal atoms in M/DV-GS (denoted as B1, B2, B3, and B4). The distance from the metal atoms to the plane of the graphene-based substrates was denoted as the elevation height of the metal atoms (H). To analyze the effect of metal atoms on catalytic performance, transition metals in the third period (Ti, V, Cr, Mn, Fe, Co, Ni, and Cu) and typical precious metals (Pd, Pt, Ag, and Au) were selected as the atoms to be embedded. In summary, there were a total of 132 catalytic structures which consisted of 11 types of graphene-based substrates and 12 types of metal atoms.

3. Results and discussion

3.1. Geometric structures

The high activity and selectivity of SACs originates in their unique geometric and electronic structure. Therefore, the bond lengths (between the metallic dopant and the adjacent atoms) and the elevation heights of the metal atoms are evaluated here. First, we summarized the bond lengths between the metal and its adjacent atoms, as shown in Tables S1–S12. From Tables S1–S12, we see that the bond lengths are in agreement with previous studies in the literature, which guarantees the accuracy of our calculated results. Second, the elevation heights of the metal atoms are plotted in Figs. 2 and 3, with data from both our calculations and the literature as shown in Tables S13 and S14.

From Fig. 2, the elevation heights of the metal atoms in the M/SV-GS are all larger than 1.2 Å, indicating that the space of the single vacancy is not large enough to hold the metal atoms in the graphene plane. The elevation height gradually decreases from Ti to Co, and Co/SV-GS has the lowest elevation height among the 12 metal atoms in the M/SV-GS. There is no clear effect of the doping of nitrogen on the elevation height of metal atoms in M/SV-GS. From Fig. 3 and Fig. S1, generally, we see that the elevation height of the metal atoms in the M/DV-GS decreases as the

amount of doped nitrogen increases, which suggests that the doping of nitrogen has a significant effect on promoting the embedding of metal atoms on DV-GS. Except for Ti and V, all of the metal atoms can be embedded in the graphene plane due to the promoting effect of doped

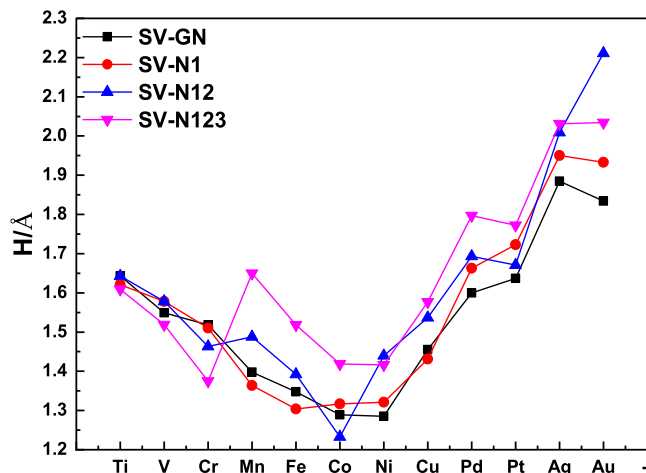


Fig. 2. The elevation heights of metal atoms in M/SV-GS.

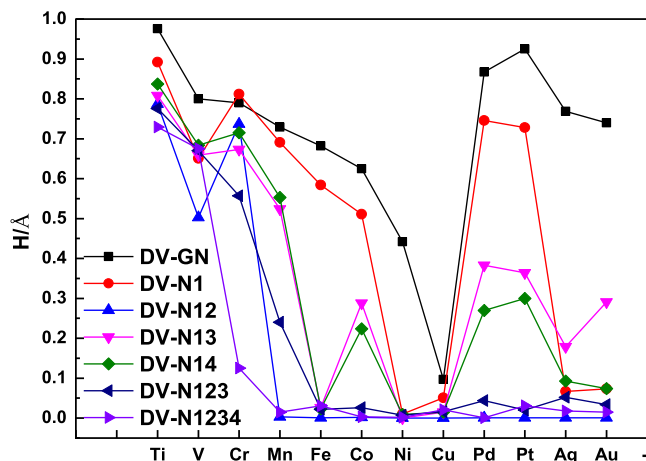


Fig. 3. The elevation heights of metal atoms in M/DV-GS.

nitrogen. Using the doped nitrogen, Cr is the first metal atom of the third period which can almost be embedded in a graphene plane (Cr/DV-N1234). As a consequence of having smallest atomic radius (1.45 Å) [74], the elevation heights of Cu in M/DV-GS are the lowest, and Cu can be directly embedded in the graphene plane without the promoting effect of nitrogen doping. Compared to M/SV-GS, the elevation heights of metal atoms in M/DV-GS are significantly lower, which can be explained by the larger space of double vacancies available to accommodate the metal atoms. Furthermore, according to Fig. S2, there was a tendency for the average elevation heights of metal atoms to increase with the increase of the atomic radius.

3.2. Electronic characteristics

3.2.1. Charge analysis

The charge of the metal atoms in M/GS (Q) is an important factor that affects catalytic activity. Liu et al. [36] have shown that the charge of the metal atoms in M/GS acts as the microscopic driving force for O_2 dissociation. According to Sun et al. [75], there is a positive correlation between the charge of metal atoms in M/GS and the dissociation energy of propane dehydrogenation. In addition, our previous study [33] indicates that there is a clear linear relationship between the charges of Fe in Fe/SV-GS and the catalytic activity of the activating O_2 . Therefore, the charge of metal atoms in M/GS are summarized in Figs. 4 and 5, with the data from our calculations and data from the literature as shown in Tables S15 and S16.

As we can see from Fig. 4, for the metal atoms in the third period, the amount of charge of the metal atoms decreases gradually with the increase of the atomic number. From Fig. 5, and similar to the charge of metal atoms in M/SV-GS, we see that there is also a downward trend in the amount of charge from Ti to Cu. Comparing the charge of the metal atoms in M/SV-GS and M/DV-GS (as shown in Fig. S3), the metal atoms in M/DV-GS are slightly larger than that the metal atoms in M/SV-GS, suggesting that the double vacancies have a promoting effect on the charges of metal atoms in graphene-based substrates. In addition, except for Ti and V, the doped nitrogen has clear promoting effect on the charge of the metal atoms.

To describe the charge of metal atoms in M/GS, electronegativity (X) was introduced as a charge descriptor based on the atoms' atomic electronegativity [76]. Given the different coordination environments in different graphene-based substrates, the contribution of atoms adjacent to the metal atom was considered. The value of X can be obtained according to the following equation:

$$X = (xX_C + yX_N - X_M) \times \frac{\theta_d}{n_d}, \quad (6)$$

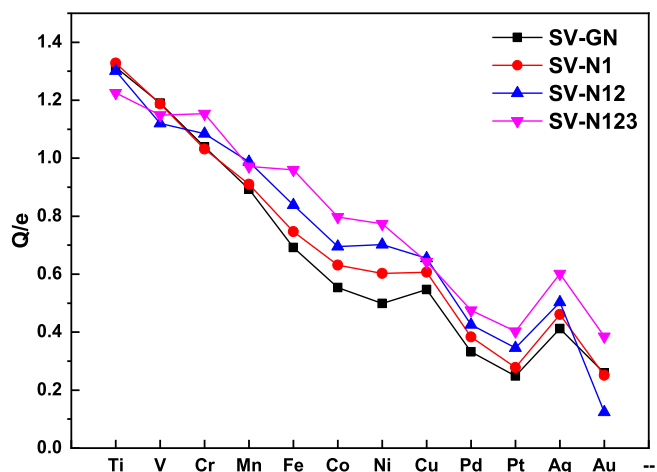


Fig. 4. The charge of metal atoms in M/SV-GS.

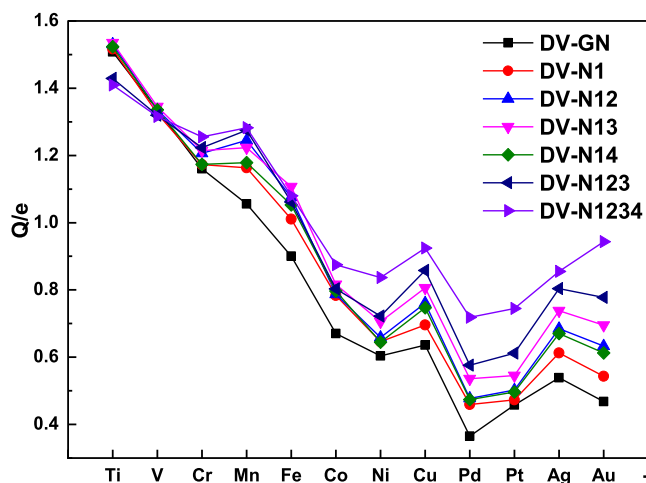


Fig. 5. The charge of metal atoms in M/DV-GS.

where x is the number of carbon atoms adjacent to the embedded metal atom, X_C is the electronegativity of the carbon atoms, y is the amount of nitrogen adjacent to the embedded metal atom, X_N is the electronegativity of the nitrogen, X_M is the electronegativity of the metal atoms, θ_d is the number of occupied electrons of the d orbitals, and n_d is the maximum number of electrons in the d orbitals. The equation of electronegativity consists of two parts: the contribution of metal atoms and the contribution of adjacent atoms.

Using Equation (6), specific values of X were calculated and are summarized in Table S17. To examine the correlation between X and Q , two types of correlations were investigated. One is the correlation between X and Q for different metal atoms with the same graphene-based substrates, and the other is the correlation between X and Q for different graphene-based substrates with the same metal atoms. Linear regressions between X and Q for different metal atoms and different graphene-based substrates were performed, as shown in Figs. 6 and 7, respectively.

In Fig. 6, a significant negative linear relationship between X and Q for different metal atoms is shown. The correlation coefficients all exceed 0.8, indicating that the descriptor of X can be used to describe the charge tendency between different metal atoms in the same graphene-based substrates. It is noteworthy that the slope of the regression line gradually decreases with the doping of nitrogen atoms, which may suggest that the sensitivity of X to Q decreases with the doping of nitrogen atoms. In Fig. 7, a clearly positive linear correlation between X and Q for different graphene-based substrates is shown (except for Ti and Ni). By examining the correlation of X and Q in different metal atoms and graphene-based substrates, we can conclude that the descriptor X , based on electronegativity, can be a good descriptor for the charge information of metal atoms in M/GS.

3.3. Investigations of d -band center

Owing to its importance in the description of catalytic activity, the d -band center (average energy of d -electrons) of M/GS was calculated and plotted in Figs. 8 and 9, and the data is summarized in Tables S18 and S19. It can be seen from Figs. 8 and 9 that there is a decreasing trend in the d -band center from Ti to Cu, which is consistent with the d -band center order of their bulk forms. However, the effect of doped nitrogen on d -band center, does not show a clear correlation between the d -band center and doping nitrogen in M/DV-GS. However, doping nitrogen caused a significant promoting effect on the d -band center in M/SV-GS ($M = Cu, Pd, Pt, Ag, \text{ and } Au$), suggesting that the catalytic activity of M/SV-GS ($M = Cu, Pd, Pt, Ag, \text{ and } Au$) can be tailored through the doping of nitrogen.

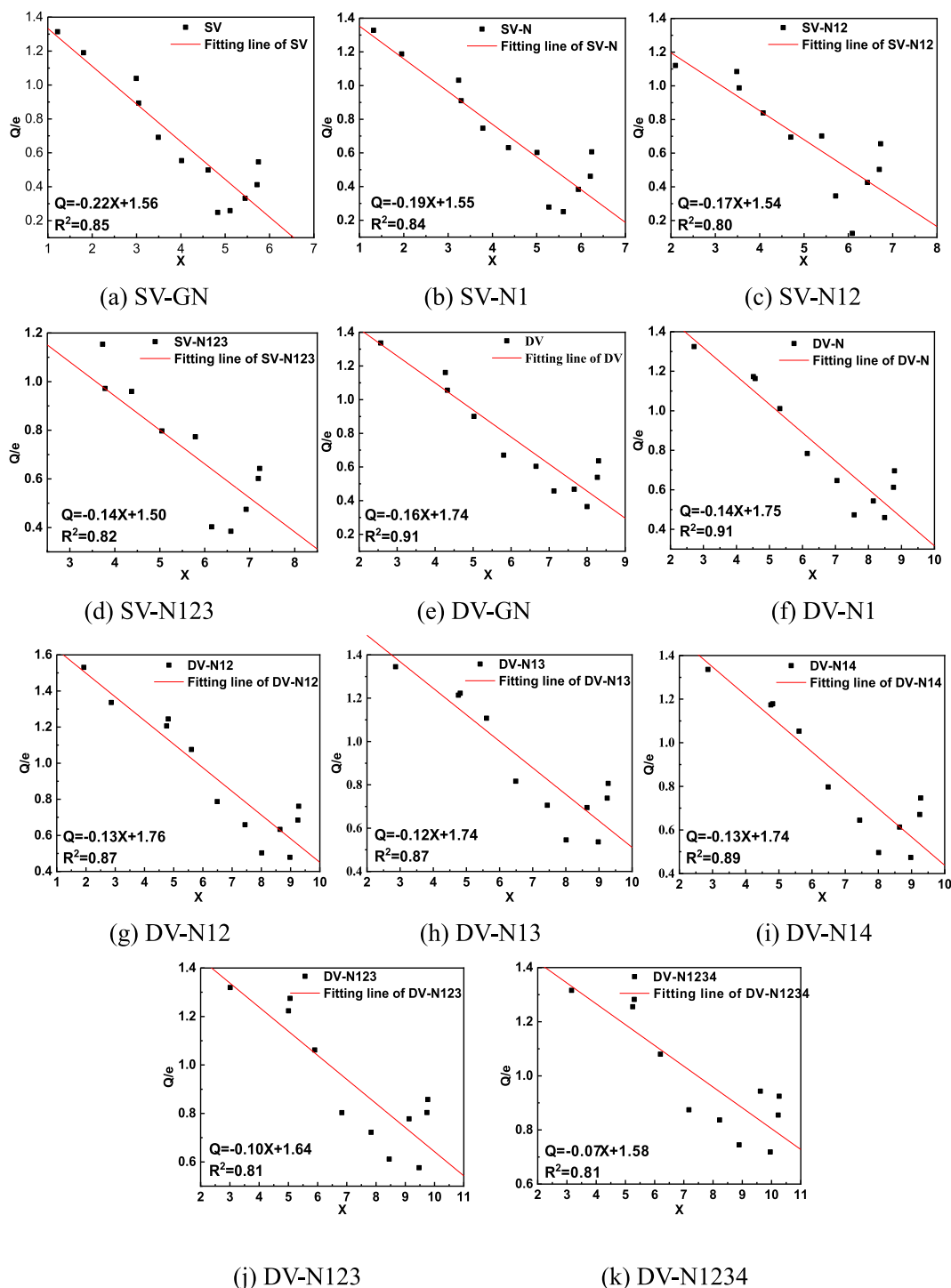


Fig. 6. Linear regressions of X and Q for different metal atoms.

3.4. Stability analysis

As mentioned above, structural stability is a key factor of SACs [77]. To investigate the stability of M/GS, the formation energy of M/GS was calculated to assess the difficulty of forming a desired structure. By comparing the formation energy with zero, we can evaluate whether the formation of the catalyst is thermodynamically favorable. Moreover, we calculated the binding energy of metal atoms on graphene-based substrate to measure the anchoring strength for metal atoms. By comparing the binding energy and the cohesive energy of metal atoms, we can estimate whether the metal atoms are likely to agglomerate.

First, we plotted the formation energies of graphene-based substrates and M/GS, as shown in Figs. 10 and 11, using the calculations from our data and from the literature, as shown in Tables S20 and S21. Fig. 10 shows that there is a clear difference in the formation energy of M/GS with different metal atoms and the same support. In M/GS with the same metal atom and different supports, the formation energy of M/GS increases as the amount of doped nitrogen increases, except for Pt, which suggests that the doped nitrogen atoms have significant promoting effects on the stability of M/GS. Among the 12 types of metal atoms, the formation energies of Ti/SV-GS are all below zero, indicating that Ti/SV-GS has higher thermodynamic stability than the other systems studied.

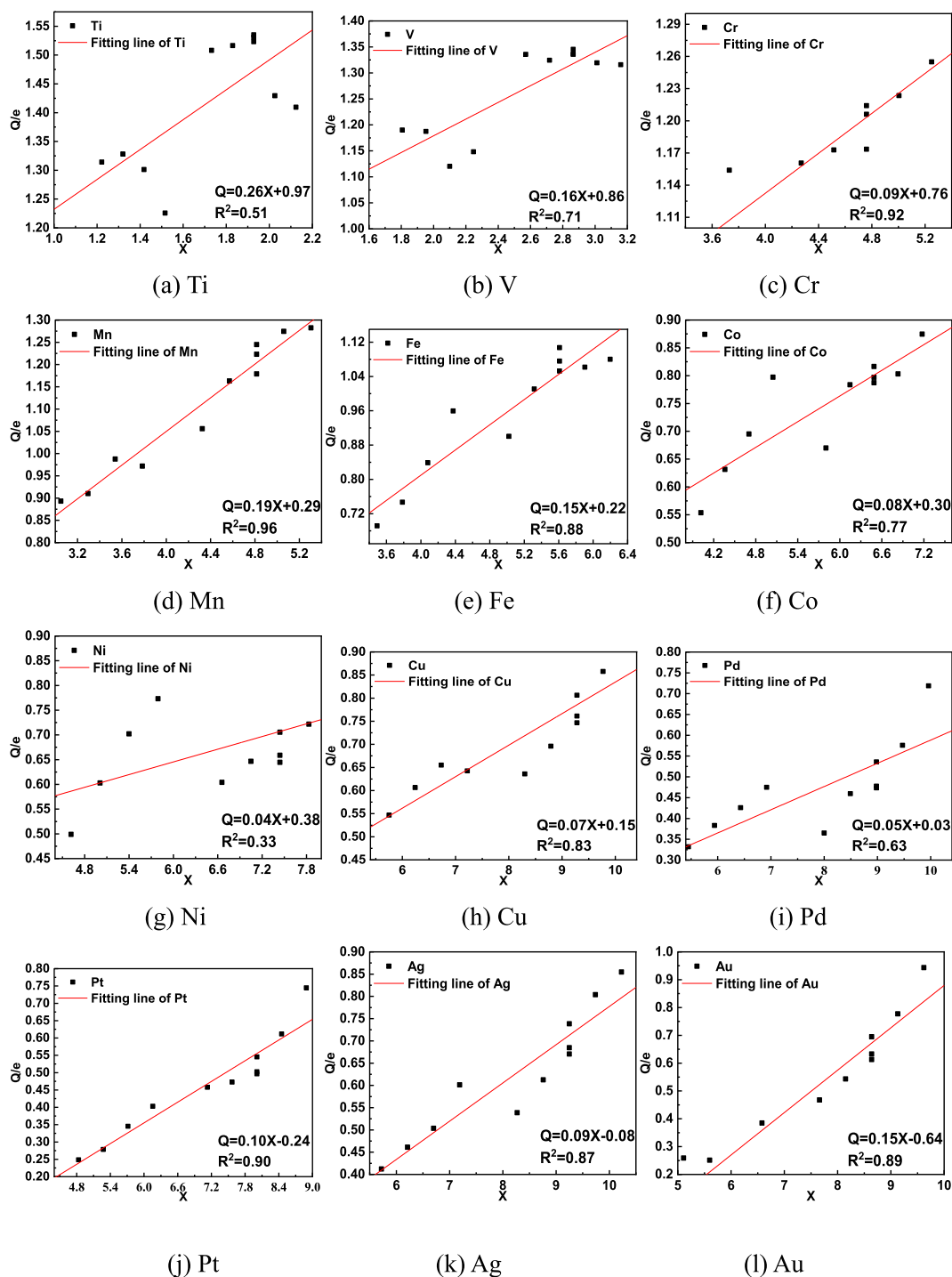


Fig. 7. Linear fitting of X and Q for different graphene-based substrates.

The formation energies of M/SV-GS (M = Cu, Pd, Pt, Ag, and Au) are all above zero, suggesting that these configurations may not remain stable. It should be noted that the formation energies of M/SV-GS (M = Fe, Co, Ni, Cu, Pd, and Pt) are all negative, as calculated by Kirk et al. [39]; the obvious differences in the formation energies between this work and that in the literature are mainly caused by the different calculation formulas. The formation energies of defects and doping were not included in Kirk et al. [39] calculations of formation energies. From the perspective of guiding catalysts' synthesis, it is plausible that the effects of both defects and doping should be considered when calculating the formation energies of M/GS. Therefore, we considered the effects of defects and doped nitrogen in our formation energy calculations.

In Fig. 11, similar to M/SV-GS, we see that the metal atoms have significant influences on the thermodynamic stability of M/DV-GS, together with the notable promoting effect of doped nitrogen atoms on the thermodynamic stability of M/DV-GS. Among the three doping configurations, when the doping used two nitrogen atoms in M/DV-GS the formation energies of the M/DV-N14 were more negative than in the other two configurations; thus, M/DV-N14 has a higher thermodynamic stability than the other two configurations. In addition, the formation energies of Ag/DV-GS and Au/DV-GS are above zero, suggesting that these configurations may not be stable. In the M/SV-GS and M/DV-GS, there was a linear relationship between the promoting effect of doped nitrogen on the thermodynamic stability of M/GS and the amount of

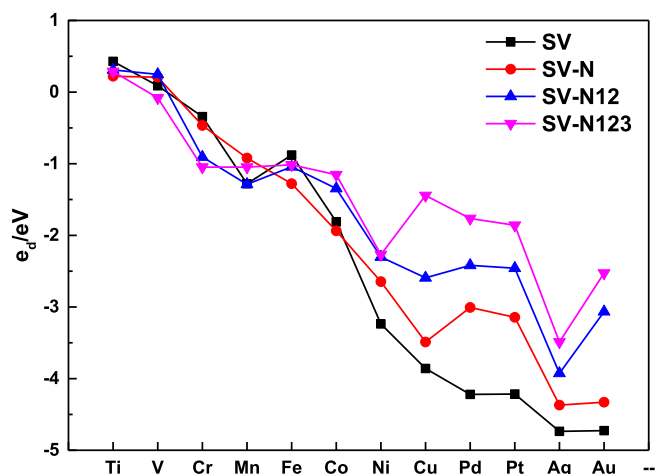


Fig. 8. Calculated d -band center of M/SV-GS.

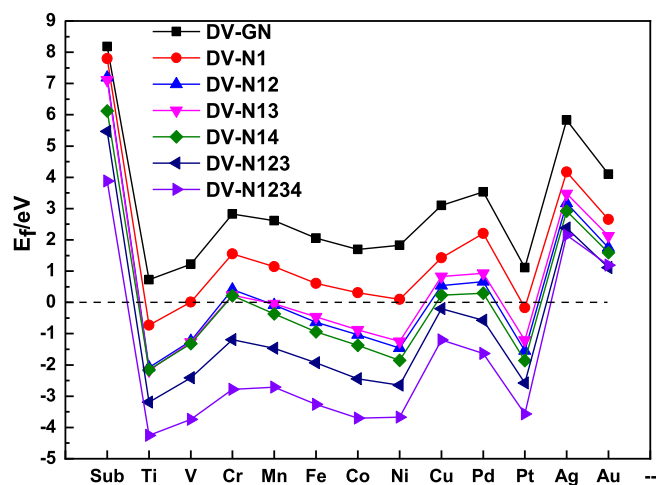


Fig. 11. Formation energies of M/DV-GS.

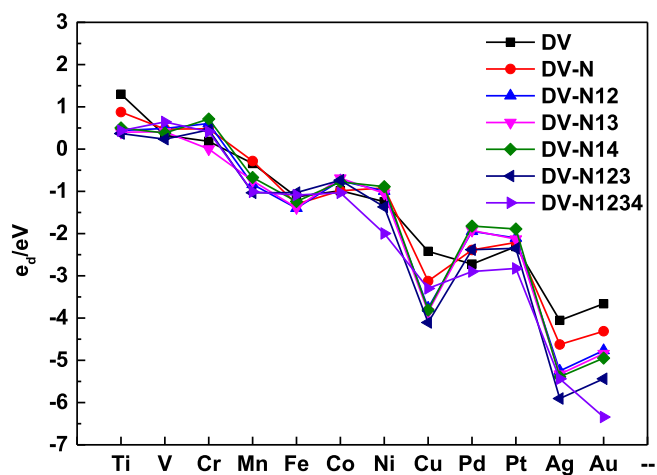


Fig. 9. Calculated d -band center of M/DV-GS.

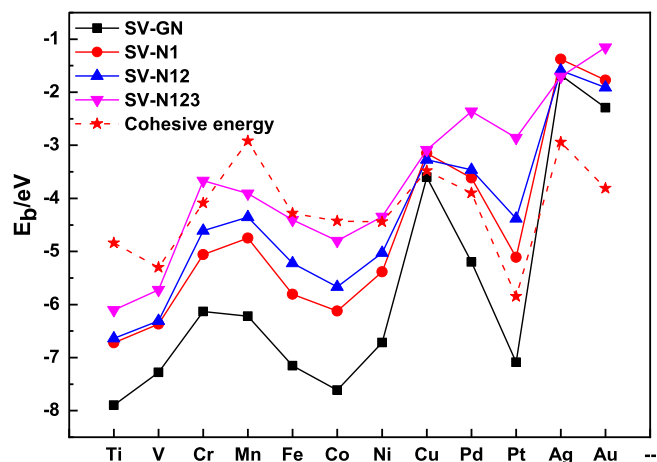


Fig. 12. Binding energies of M/SV-GS.

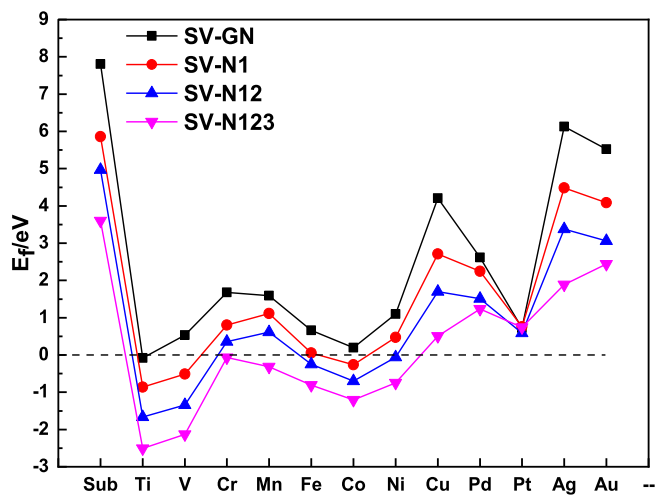


Fig. 10. Formation energies of M/SV-GS.

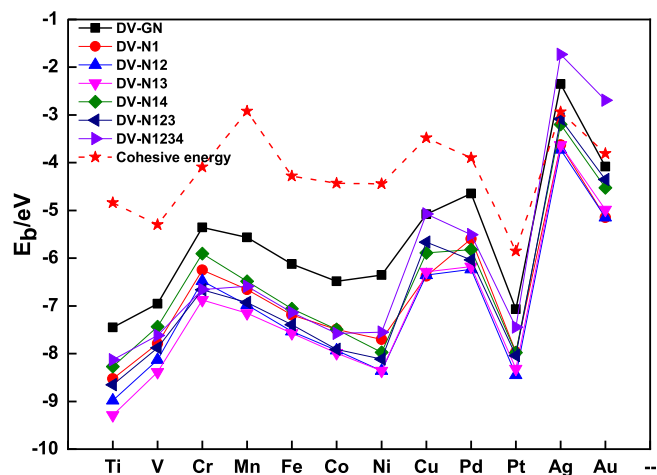


Fig. 13. Binding energies of M/DV-GS.

doped nitrogen, indicating the promoting effect of greater numbers of doped nitrogen atoms.

Second, we plotted the binding energies of M/GS as shown in Figs. 12 and 13, with the results of our detailed calculations and those from the literature are provided in Tables S22 and S23. In Figs. 12 and 13, the reference values of the cohesive energies of different metal atoms are

labeled as stars. Fig. 12 shows that the binding energies of M/GS are all below zero, which indicates that the metal atoms can be adsorbed on the surface of graphene-based substrates. Regarding the effects of the doped nitrogen atoms, the binding energies of M/SV-GS decreases as the number of doped nitrogen atoms increases, revealing that the doping of

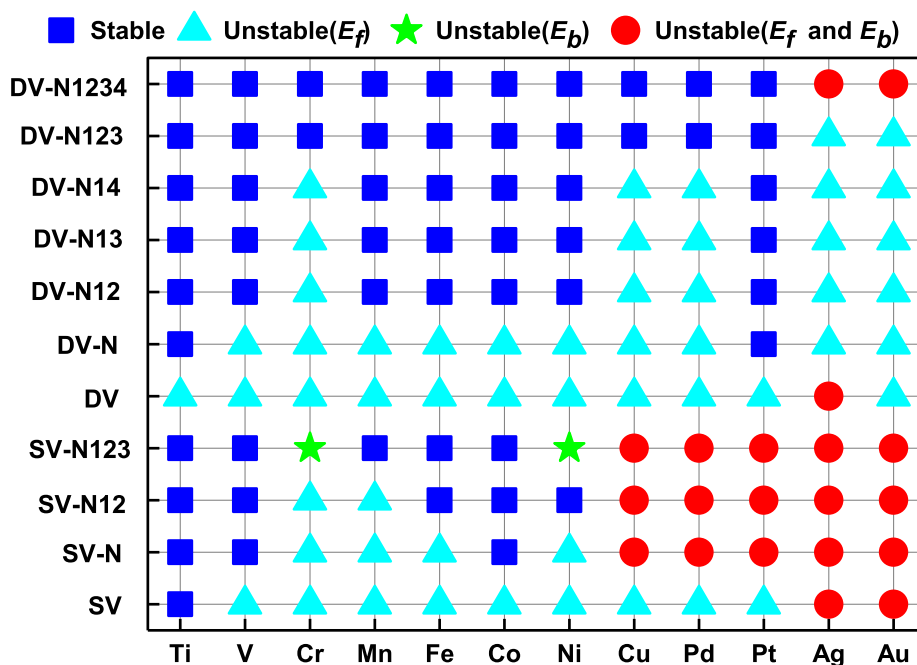


Fig. 14. Stability map of M/GS in formation and agglomeration. Blue squares represent the stable configurations in formation and agglomeration. Red circles represent the unstable configurations in both formation and agglomeration. Cyan triangles indicate that the configuration is unstable with respect to formation. Green stars indicate that the configuration is unstable with respect to agglomeration.

nitrogen has an inhibitory effect on the adsorption of metal atoms. Specifically, the binding energies of Ag/SV-GS and Au/SV-GS are all above their corresponding cohesive energies, which suggests that Ag/SV-GS and Au/SV-GS are likely to agglomerate and form micro clusters.

In Fig. 13, we can see that the binding energies of M/DV-GS are almost below the corresponding cohesive energies, indicating that the anchoring effect of double vacancies in the graphene-based substrates on metal atoms is strong enough to prevent agglomeration. As compared to M/SV-GS, the double vacancy graphene-based substrates anchor the metal atoms more firmly. Specifically, the binding energies of M/DV-GS combined with the doped nitrogen are almost below the binding energies in the samples without nitrogen doping, which means that the doping of nitrogen can strengthen the binding energies of M/DV-GS. However, we did not find a clear linear relationship between the amount of doped nitrogen and the binding energy. It is worth noting that the doping of nitrogen atoms has two opposite effects on the binding energies in M/SV-GS and M/DV-GS, namely a suppressing effect on M/SV-GS and a promoting effect on M/DV-GS. The different effects of nitrogen doping may originate in the type of bonding between metal atoms and the adjacent atoms, needs further study.

Based on the calculations of the formation energies and binding energies, the configurations of M/GS are labeled using different colors and symbols, as shown in Fig. 14. According to the properties of formation and agglomeration, 57 potentially stable configurations were revealed in the 132 types of M/GS. In Fig. 14, we see that the configurations of Ag-GS and Au-GS are all unstable, which indicates that Ag and Au may not be suitable as embedding metals for SACs supported with graphene-based substrates. Comparing M/SV-GS with M/DV-GS, we see that there are more stable configurations in M/DV-GS than in M/SV-GS, indicating that double vacancy graphene-based substrates are more suitable for use as a catalytic support. In terms of the catalyst preparation, the configurations of M/DV-N1234 (M = Fe, Co, and Ni) are all stable as shown in this stability map, and those configurations have also been successfully synthesized in substantial experiments [78]. Although many theoretical studies have reported on Pd/SV [35,64,79,80] and Pt/SV [31,36,81], studies on the preparation of Pd/SV and Pt/SV in experiment are rarely discussed. According to our stability map, the configurations of Pd/SV

and Pt/SV are all unstable which may cause the difficulties during synthesis. We expect that this stability map of M/GS can provide some theoretical guidance for the screening and preparation of catalysts.

3.5. Catalytic activity screening

The DFT calculation facilitates the prediction of catalytic activity based on calculated geometric structures and their electronic characteristics. According to the theoretical research of Huang et al. [82], there is an obvious linear relationship between the magnetic moment of metal atoms and overpotential in the system of single-atom Fe catalysts supported with single vacancy graphene-based substrates, and the higher magnetic moment of metal atoms corresponding to the higher catalytic

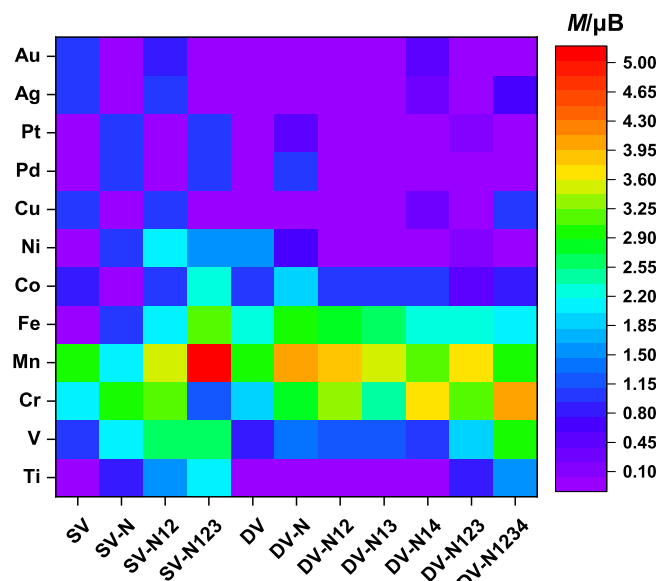


Fig. 15. Magnetic moment map of M/GS for nitrogen reduction reaction.

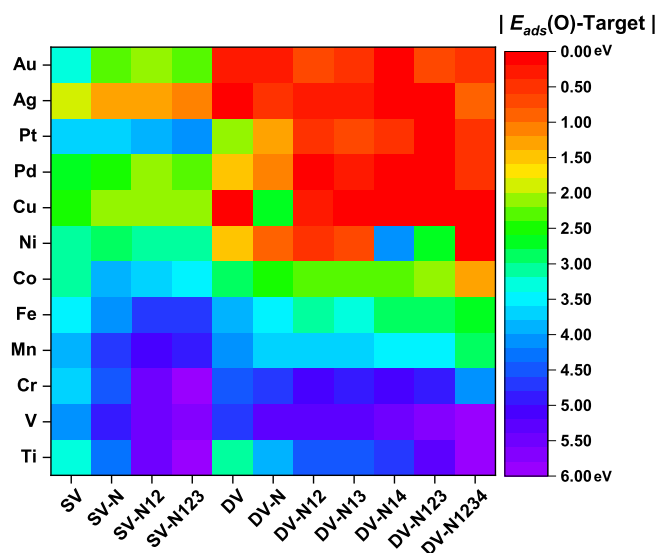


Fig. 16. Relative O atom adsorption energy map of M/GS for ORR.

activity of the nitrogen reduction reaction (NRR). Therefore, based on this theoretical conclusion, we calculated the magnetic moment of metal atoms in the 132 M/GS to predict the catalytic activity of M/GS for NRR. The calculation data of the magnetic moments are plotted in Fig. 15, and the values are summarized in Table S24. Significantly, among the 132 M/GS, the magnetic moment of Mn/SV-N123 is the highest, indicating that Mn/SV-N123 may have a relatively higher catalytic activity of NRR. In addition, the magnetic moment of Fe/SV-N123 is relatively large, and Fe/SV-N123 has a high catalytic activity of NRR, which has been proved by the experimental research of Wang et al. [83].

In addition, the adsorption strength of the simple adsorbate on the surface of the catalyst has been used to predict catalytic activity and selectivity [45–47,84,85]. In particular, based on the adsorption energy of O on a catalytic surface, the activity of catalysts in an oxygen reduction reaction (ORR) [86–88] and ethylene epoxidation [47,89,90] were successfully predicted. Therefore, we calculated the adsorption energies of O on the 132 M/GS, as shown in Table S24. According to the volcano model of ORR by Nørskov et al. [91], the adsorption energy of O can be a simple

and effective descriptor of the catalytic activity in an ORR. Based on the calculated adsorption energies of O atoms on the M/GS, we predicted their catalytic activities in ORR utilizing the conclusion of the volcano model. To facilitate the calculation of catalytic activity, the adsorption energy of O atom on a pure Pt surface (1.57 eV) was selected as the target catalyst, following previous studies [91–93], with the assumption that the smaller difference between $E_{ads}(O)$ on M/GS and the Pt surface would lead to higher ORR activity. Based on this, the ORR catalytic activity map for the 132 M/GS is plotted in Fig. 16. According to this relative O atom adsorption energy map of M/GS, we can predict that Ni/DV-N1234, Cu/DV, Cu/DV-N13, Cu/DV-N14, Cu/DV-N123, Cu/DV-N1234, Pt/DV-123, Ag/DV, Ag/DV-N14, and Ag/DV-N123 are all promising catalysts for ORR. Furthermore, considering the stability of the catalyst (Fig. 8), Ni/DV-N1234 [6], Cu/DV-N123, and Pt/DV-N123 should be experimentally tested; it is worth trying to apply these catalysts to perform ORR. In addition, Cu/DV-N1234 has been proven to be an effective catalyst for ORR in the experiments done by Baek et al. [94], which further verifies that our predictions are reliable. We also expect that these descriptor-based screening methods for SACs will also be effective for other types of catalysis, such as hydrogen evolution [95], oxygen evolution [96], and nitrite reduction [97].

3.6. Descriptor of adsorption energy

To further accelerate the development of catalysts, we studied a simple and effective descriptor for O adsorption energy based on the bonding mechanism. Given that bond hybridization and electron transfer could occur simultaneously in the formation of chemical bonds on the surface of catalysts [98], there should be two contributions to the adsorption energies: the contribution of bond hybridization and the contribution of electron transfer. The contribution of bond hybridization and electron transfer to adsorption energies can be related to the d -band center of a catalytic surface (ϵ_d) and the electronegativity (X), respectively. Therefore, ϵ_d and X were adopted to describe the adsorption energies of oxygen on all the M/GS studied. The E_{ads} of O on different M/GS surfaces were fitted with ϵ_d and X using the two-dimensional (2D) polynomial model shown in Fig. 17.

It can be seen from Fig. 17 that the data points of E_{ads} are almost distributed near the fitting plane with an R^2 of 0.83, suggesting that the model of $E_{ads}-(\epsilon_d, X)$ can be an effective descriptor of the oxygen

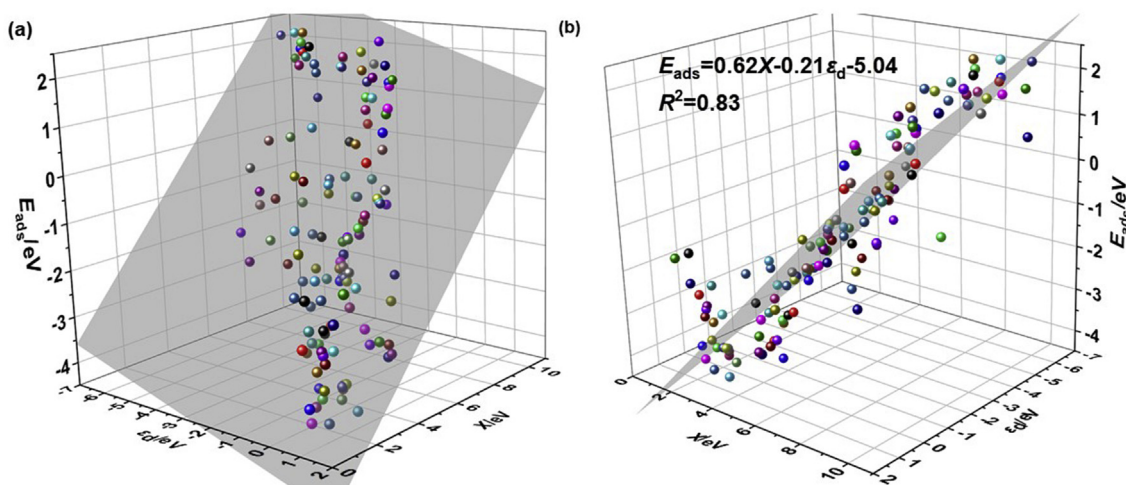


Fig. 17. (a) Top and (b) side views of $E_{ads}-(\epsilon_d, X)$ and the 2D polynomial fitting.

adsorption. The fitted equation is $E_{\text{ads}} = 0.62X - 0.21\epsilon_d - 5.04$, which indicates that the smaller the electronegativity and the larger the d -band center, the greater the adsorption strength. In the adsorption on the surface of M/GS, oxygen always gains electrons, so a small electronegativity could promote charge transfer and favors the adsorption of oxygen. Regarding the relationship between adsorption energy and d -band center, according to the method of d -band center [51,76,99], a higher d -band center location (less electrons in the d -orbital) results in anti-bonding states with a higher level of d -band center and lower occupancy of anti-bonding states, leading to the stronger interaction between the adsorbate and the catalyst's surface. Therefore, the fitted equation is in accordance with the previous theory of electronegativity and d -band center, which confirms that the model of $E_{\text{ads}}(\epsilon_d, X)$ contains useful physical insights. Compared to the model of work function with d -band center proposed by Shen et al. [98], the complex work function calculation can be replaced by a simple electronegativity calculation in the model of $E_{\text{ads}}(\epsilon_d, X)$, which allows us to calculate accurate adsorption energies of oxygen with the lowest computation costs. Furthermore, we expect that the $E_{\text{ads}}(\epsilon_d, X)$ model can provide sufficient theoretical guidance for the design of catalysts with high catalytic activity and selectivity.

4. Conclusions

In this paper, the structures, charge, stability, adsorption energy, catalytic activity, and descriptors for 132 types of single-atom catalysts supported on different graphene substrates were evaluated using DFT calculations. Based on the formation and binding energies, a stability map of M/GS was developed, which can guide catalyst synthesis from the perspectives of thermodynamic stability and agglomeration. We have discussed the effects of metal atoms and supports on the charge of the metal atoms and their stability. We have found that the doping of nitrogen on graphene-based substrates can significantly promote the thermodynamic stability of M/GS. Based on the catalytic screening and structural stability results, we suggest that Ni/DV-N1234, Cu/DV-N123 and Pt/DV-N123 are promising catalysts for ORR, while Mn/SV-N123 is a potential catalyst for NRR. The electronegativity of M/GS can describe the variation of metal atom charge in different metal atoms and substrates. Combined with the electronegativity and d -band center, a simple but effective descriptor of M/GS was proposed to predict the adsorption energy of O on M/GS, which is expected to significantly lower the time needed for theoretical screening of promising catalysts. Furthermore, we expect that this comprehensive research will provide an important predictive guide, in the view of the stability and catalytic activity results observed, for both the synthesis and rational design of single-atom catalysts.

Acknowledgements

This work was supported by the National Natural Science Foundation of China (No. 91545122), Beijing Natural Science Foundation (2182066), Natural Science Foundation of Hebei Province of China (B2018502067), and the Fundamental Research Funds for the Central Universities (2017XS121). IDG and CCW acknowledge support from the University of Calgary's Canada First Research Excellence Fund (CFREF) program entitled the Global Research Initiative for Sustainable Low Carbon Unconventional Resources.

Appendix A. Supplementary data

Supplementary data to this article can be found online at <https://doi.org/10.1016/j.nanoms.2019.10.008>.

References

- [1] L. Liu, A. Corma, Metal catalysts for heterogeneous catalysis: from single atoms to nanoclusters and nanoparticles, *Chem. Rev.* 118 (10) (2018) 4981–5079.
- [2] H. Li, W. Chai, G. Henkelman, Selectivity for ethanol partial oxidation: the unique chemistry of single-atom alloy catalysts on Au, Ag, and Cu (111), *J. Mater. Chem. A* 7 (41) (2019) 23868–23877.
- [3] B. Qiao, A. Wang, X. Yang, L.F. Allard, Z. Jiang, Y. Cui, J. Liu, J. Li, T. Zhang, Single-atom catalysis of CO oxidation using Pt1/FeOx, *Nat. Chem.* 3 (8) (2011) 634–641.
- [4] L. Wang, W. Zhang, S. Wang, Z. Gao, Z. Luo, X. Wang, R. Zeng, A. Li, H. Li, M. Wang, X. Zheng, J. Zhu, W. Zhang, C. Ma, R. Si, J. Zeng, Atomic-level insights in optimizing reaction paths for hydroformylation reaction over Rh/CoO single-atom catalyst, *Nat. Commun.* 7 (2016) 14036.
- [5] C. Wu, K.M.K. Yu, F. Liao, N. Young, P. Nellist, A. Dent, A. Kroner, S.C.E. Tsang, A non-syn-gas catalytic route to methanol production, *Nat. Commun.* 3 (2012) 1050.
- [6] H. Fei, J. Dong, Y. Feng, C.S. Allen, C. Wan, B. Voloskiy, M. Li, Z. Zhao, Y. Wang, H. Sun, P. An, W. Chen, Z. Guo, C. Lee, D. Chen, I. Shakir, M. Liu, T. Hu, Y. Li, A.I. Kirkland, X. Duan, Y. Huang, General synthesis and definitive structural identification of MN4C4 single-atom catalysts with tunable electrocatalytic activities, *Nat. Catal.* 1 (1) (2018) 63–72.
- [7] W. Liu, L. Zhang, W. Yan, X. Liu, X. Yang, S. Miao, W. Wang, A. Wang, T. Zhang, Single-atom dispersed Co-N-C catalyst: structure identification and performance for hydrogenative coupling of nitroarenes, *Chem. Sci.* 7 (9) (2016) 5758–5764.
- [8] H. Fei, J. Dong, M.J. Arellano-Jimenez, G. Ye, N.D. Kim, E.L.G. Samuel, Z. Peng, Z. Zhu, F. Qin, J. Bao, M.J. Yacaman, P.M. Ajayan, D. Chen, J.M. Tour, Atomic cobalt on nitrogen-doped graphene for hydrogen generation, *Nat. Commun.* 6 (2015) 8668.
- [9] D. Deng, X. Chen, L. Yu, X. Wu, Q. Liu, Y. Liu, et al., A single iron site confined in a graphene matrix for the catalytic oxidation of benzene at room temperature, *Sci. Adv.* 1 (11) (2015), e1500462.
- [10] Y. Li, Z. Zhou, G. Yu, W. Chen, Z. Chen, CO catalytic oxidation on iron-embedded graphene: computational quest for low-cost nanocatalysts, *J. Phys. Chem. C* 114 (14) (2010) 6250–6254.
- [11] M.D. Esrafil, S. Heydari, CO oxidation catalyzed by a single Ti atom supported on divacancy defective graphene: a dispersion-corrected DFT study, *ChemistrySelect* 3 (16) (2018) 4471–4479.
- [12] M. Zhao, R. Zhao, M. Niu, W. Li, Y. Ma, Y. Li, Y. Tang, X. Dai, Promotion of CO oxidation on the Fe/Nx clusters embedded graphene, *Appl. Phys. A-Mater.* 123 (3) (2017).
- [13] W. Rui, F. Wei, Z. Dandan, L. Huiling, Z. Huanan, H. Xuri, Geometric stability of PtFe/PdFe embedded in graphene and catalytic activity for CO oxidation, *Appl. Organomet. Chem.* 31 (11) (2017), e3808.
- [14] X. Zhang, Z. Lu, Z. Yang, Single non-noble-metal cobalt atom stabilized by pyridinic vacancy graphene: an efficient catalyst for CO oxidation, *J. Mol. Catal. A Chem.* 417 (2016) 28–35.
- [15] Y. Liu, H. Li, W. Cen, J. Li, Z. Wang, G. Henkelman, A computational study of supported Cu-based bimetallic nanoclusters for CO oxidation, *Phys. Chem. Chem. Phys.* 20 (11) (2018) 7508–7513.
- [16] C. Yan, H. Li, Y. Ye, H. Wu, F. Cai, R. Si, J. Xiao, S. Miao, S. Xie, F. Yang, Y. Li, G. Wang, X. Bao, Coordinatively unsaturated nickel-nitrogen sites towards selective and high-rate CO2 electroreduction, *Energy Environ. Sci.* 11 (5) (2018) 1204–1210.
- [17] C. Zhang, S. Yang, J. Wu, M. Liu, S. Yazdi, M. Ren, J. Sha, J. Zhong, K. Nie, A.S. Jallilov, Z. Li, H. Li, B.I. Yakobson, Q. Wu, E. Ringe, H. Xu, P.M. Ajayan, J.M. Tour, Electrochemical CO2 reduction with atomic iron-dispersed on nitrogen-doped graphene, *Adv. Energy Mater.* 8 (19) (2018) 1703487.
- [18] H. He, Y. Jagvaral, Electrochemical reduction of CO2 on graphene supported transition metals- towards single atom catalysts, *Phys. Chem. Chem. Phys.* 19 (18) (2017) 11436–11446.
- [19] X. Guo, S. Liu, S. Huang, Single Ru atom supported on defective graphene for water splitting: DFT and microkinetic investigation, *Int. J. Hydrogen Energy* 43 (10) (2018) 4880–4892.
- [20] L. Liu, C. Chen, L. Zhao, Y. Wang, X. Wang, Metal-embedded nitrogen-doped graphene for H2O molecule dissociation, *Carbon* 115 (2017) 773–780.
- [21] Y. Chen, S. Ji, Y. Wang, J. Dong, W. Chen, Z. Li, R. Shen, L. Zheng, Z. Zhuang, D. Wang, Y. Li, Isolated single iron atoms anchored on N-doped porous carbon as an efficient electrocatalyst for the oxygen reduction reaction, *Angew. Chem. Int. Ed.* 56 (24) (2017) 6937–6941.
- [22] X. Chen, L. Yu, S. Wang, D. Deng, X. Bao, Highly active and stable single iron site confined in graphene nanosheets for oxygen reduction reaction, *Nano Energy* 32 (2017) 353–358.
- [23] G. Vile, D. Albani, M. Nachtegaal, Z. Chen, D. Dontsova, M. Antonietti, N. Lopez, J. Perez-Ramirez, A stable single-site palladium catalyst for hydrogenations, *Angew. Chem. Int. Ed.* 54 (38) (2015) 11265–11269.
- [24] J. Liu, Catalysis by supported single metal atoms, *ACS Catal.* 7 (1) (2017) 34–59.
- [25] S. Liang, C. Hao, Y. Shi, The power of single-atom catalysis, *ChemCatChem* 7 (17) (2015) 2559–2567.
- [26] X. Yang, A. Wang, B. Qiao, J. Li, J. Liu, T. Zhang, Single-atom catalysts: a new frontier in heterogeneous catalysis, *Accounts Chem. Res.* 46 (8) (2013) 1740–1748.
- [27] K. Niu, B. Yang, J. Cui, J. Jin, X. Fu, Q. Zhao, J. Zhang, Graphene-based non-noble-metal Co/N/C catalyst for oxygen reduction reaction in alkaline solution, *J. Power Sources* 243 (2013) 65–71.
- [28] L. Fan, P. Liu, X. Yan, L. Gu, Z. Yang, H. Yang, S. Qiu, X. Yao, Atomically isolated nickel species anchored on graphitized carbon for efficient hydrogen evolution electrocatalysis, *Nat. Commun.* 7 (2016) 10667.

- [29] L. Jiao, G. Wan, R. Zhang, H. Zhou, S. Yu, H. Jiang, From metal-organic frameworks to single-atom Fe implanted N-doped porous carbons: efficient oxygen reduction in both alkaline and acidic media, *Angew. Chem. Int. Ed.* 57 (28) (2018) 8525–8529.
- [30] Z. Li, D. Wang, Y. Wu, Y. Li, Recent advances in the precise control of isolated single-site catalysts by chemical methods, *Natl. Sci. Rev.* 5 (5) (2018) 673–689.
- [31] X. Liu, Y. Sui, T. Duan, C. Meng, Y. Han, CO oxidation catalyzed by Pt-embedded graphene: a first-principles investigation, *Phys. Chem. Chem. Phys.* 16 (43) (2014) 23584–23593.
- [32] X. Liu, Y. Sui, T. Duan, C. Meng, Y. Han, Monodisperse Pt atoms anchored on N-doped graphene as efficient catalysts for CO oxidation: a first-principles investigation, *Catal. Sci. Technol.* 5 (3) (2015) 1658–1667.
- [33] Z. Gao, W. Yang, X. Ding, G. Lv, W. Yan, Support effects on adsorption and catalytic activation of O₂ in single atom iron catalysts with graphene-based substrates, *Phys. Chem. Chem. Phys.* 20 (10) (2018) 7333–7341.
- [34] X. Zhang, S. Yu, H. Chen, W. Zheng, TM atoms on B/N doped defective graphene as a catalyst for oxygen reduction reaction: a theoretical study, *RSC Adv.* 5 (101) (2015) 82804–82812.
- [35] A.V. Krasheninnikov, P.O. Lehtinen, A.S. Foster, P. Pyykko, R.M. Nieminen, Embedding transition-metal atoms in graphene: structure, bonding, and magnetism, *Phys. Rev. Lett.* 102 (12) (2009) 126807.
- [36] S. Liu, S. Huang, Theoretical insights into the activation of O₂ by Pt single atom and Pt₄ nanocluster on functionalized graphene support: critical role of Pt positive polarized charges, *Carbon* 115 (2017) 11–17.
- [37] P. Janthon, S.M. Kozlov, F. Vines, J. Limtrakul, F. Illas, Establishing the accuracy of broadly used density functionals in describing bulk properties of transition metals, *J. Chem. Theory Comput.* 9 (3) (2013) 1631–1640.
- [38] J. Zhang, Y. Wang, Y. Wang, M. Zhang, Catalytic activity for oxygen reduction reaction on CoN₂ embedded graphene: a density functional theory study, *J. Electrochem. Soc.* 164 (12) (2017) F1122–F1129.
- [39] C. Kirk, L. Chen, S. Siahrostami, M. Karamad, M. Bajdich, J. Voss, J.K. Nørskov, K. Chan, Theoretical investigations of the electrochemical reduction of CO on single metal atoms embedded in graphene, *ACS Cent. Sci.* 3 (12) (2017) 1286–1293.
- [40] M. Kaukonen, A.V. Krasheninnikov, E. Kauppinen, R.M. Nieminen, Doped graphene as a material for oxygen reduction reaction in hydrogen fuel cells: a computational study, *ACS Catal.* 3 (2) (2013) 159–165.
- [41] W. Sun, R. Shi, X. Wang, S. Liu, X. Han, C. Zhao, Z. Li, J. Ren, Density-functional theory study of dimethyl carbonate synthesis by methanol oxidative carbonylation on single-atom Cu₁/graphene catalyst, *Appl. Surf. Sci.* 425 (2017) 291–300.
- [42] J. Zhang, Y. Wang, Z. Zhu, M. Zhang, Electrochemical oxygen reduction mechanism on FeN₂-graphene, *J. Mol. Model.* 23 (5) (2017) 170.
- [43] F. Abild-Pedersen, J. Greeley, J. Studt, J. Rossmeisl, T.R. Munter, P.G. Moses, E. Skulason, T. Bligaard, J.K. Nørskov, Scaling properties of adsorption energies for hydrogen-containing molecules on transition-metal surfaces, *Phys. Rev. Lett.* 99 (1) (2007), 016105.
- [44] F. Mehmood, R.B. Rankin, J. Greeley, L.A. Curtiss, Trends in methanol decomposition on transition metal alloy clusters from scaling and Brønsted-Evans-Polanyi relationships, *Phys. Chem. Chem. Phys.* 14 (24) (2012) 8644–8652.
- [45] T. Bligaard, J.K. Nørskov, S. Dahl, J. Matthiesen, C.H. Christensen, J. Sehested, The Brønsted-Evans-Polanyi relation and the volcano curve in heterogeneous catalysis, *J. Catal.* 224 (1) (2004) 206–217.
- [46] M.M. Montemore, J.W. Medlin, Scaling relations between adsorption energies for computational screening and design of catalysts, *Catal. Sci. Technol.* 4 (11) (2014) 3748–3761.
- [47] M.M. Montemore, J.W. Medlin, Predicting and comparing C-M and O-M bond strengths for adsorption on transition metal surfaces, *J. Phys. Chem. C* 118 (5) (2014) 2666–2672.
- [48] M.M. Montemore, J.W. Medlin, A unified picture of adsorption on transition metals through different atoms, *J. Am. Chem. Soc.* 136 (26) (2014) 9272–9275.
- [49] P. Ferrin, D. Simonetti, S. Kandoi, E. Kunkes, J.A. Dumesic, J.K. Nørskov, M. Mavrikakis, Modeling ethanol decomposition on transition metals: a combined application of scaling and Brønsted-Evans-Polanyi relations, *J. Am. Chem. Soc.* 131 (16) (2009) 5809–5815.
- [50] H. Li, E.J. Evans, C.B. Mullins, G. Henkelman, Ethanol decomposition on Pd-Au alloy catalysts, *J. Phys. Chem. C* 122 (38) (2018) 22024–22032.
- [51] B. Hammer, J.K. Nørskov, Theoretical surface science and catalysis—calculations and concepts, *Adv. Catal.* 45 (2000) 71–129.
- [52] M. Qiu, Z. Fang, Y. Li, J. Zhu, X. Huang, K. Ding, W. Chen, Y. Zhang, First-principles investigation of the activation of CO₂ molecule on TM/Cu (TM=Fe, Co and Ni) surface alloys, *Appl. Surf. Sci.* 353 (30) (2015) 902–912.
- [53] X. Xia, J.L.R. Yates, G. Jones, M. Sarwar, I. Harkness, D. Thompsett, Theoretical exploration of novel catalyst support materials for fuel cell applications, *J. Mater. Chem. A* 4 (39) (2016) 15181–15188.
- [54] J. Shin, J.-H. Choi, P.-R. Cha, S.K. Kim, I. Kim, S.-C. Lee, D.S. Jeong, Catalytic activity for oxygen reduction reaction on platinum-based core-shell nanoparticles: all-electron density functional theory, *Nanoscale* 7 (38) (2015) 15830–15839.
- [55] B. Xing, G. Wang, Insight into the general rule for the activation of the X-H bonds (X = C, N, O, S) induced by chemisorbed oxygen atoms, *Phys. Chem. Chem. Phys.* 16 (6) (2014) 2621–2629.
- [56] H. Li, K. Shin, G. Henkelman, Effects of ensembles, ligand, and strain on adsorbate binding to alloy surfaces, *J. Chem. Phys.* 149 (17) (2018) 174705.
- [57] E. Evans, H. Li, W. Yu, G. Mullen, G. Henkelman, C. Mullins, Mechanistic insights on ethanol dehydrogenation on Pd-Au model catalysts: a combined experimental and DFT study, *Phys. Chem. Chem. Phys.* 19 (45) (2017) 30578–30589.
- [58] W. Yang, Z. Gao, X. Ding, G. Lv, W. Yan, The adsorption characteristics of mercury species on single atom iron catalysts with different graphene-based substrates, *Appl. Surf. Sci.* 455 (2018) 940–951.
- [59] H. Li, Z. Zhang, Z. Liu, Non-monotonic trends of hydrogen adsorption on single atom doped g-C₃N₄, *Catalysts* 9 (1) (2019) 84.
- [60] Y. Peng, Z. Geng, S. Zhao, L. Wang, H. Li, X. Wang, X. Zheng, J. Zhu, Z. Li, R. Si, J. Zeng, Pt single atoms embedded in the surface of Ni nanocrystals as highly active catalysts for selective hydrogenation of nitro compounds, *Nano Lett.* 18 (6) (2018) 3785–3791.
- [61] G. Kresse, D. Joubert, From ultrasoft pseudopotentials to the projector augmented-wave method, *Phys. Rev. B* 59 (3) (1999) 1758–1775.
- [62] J.P. Perdew, K. Burke, M. Ernzerhof, Generalized gradient approximation made simple, *Phys. Rev. Lett.* 77 (18) (1996) 3865–3868.
- [63] G. Kresse, J. Furthmüller, Efficient iterative schemes for ab initio total-energy calculations using a plane-wave basis set, *Phys. Rev. B* 54 (16) (1996) 11169–11186.
- [64] G. Xu, R. Wang, F. Yang, D. Ma, Z. Yang, Z. Lu, CO oxidation on single Pd atom embedded defect-graphene via a new termolecular Eley-Rideal mechanism, *Carbon* 118 (2017) 35–42.
- [65] Y. Tang, W. Chen, Z. Shen, C. Li, D. Ma, X. Dai, Computational study of CO oxidation reactions on metal impurities in graphene divacancies, *Phys. Chem. Chem. Phys.* 20 (4) (2018) 2284–2295.
- [66] Y. Tang, J. Zhou, Z. Shen, W. Chen, C. Li, X. Dai, High catalytic activity for CO oxidation on single Fe atom stabilized in graphene vacancies, *RSC Adv.* 6 (96) (2016) 93985–93996.
- [67] X. Zhang, Z. Lu, G. Xu, T. Wang, D. Ma, Z. Yang, L. Yang, Single Pt atom stabilized on nitrogen doped graphene: CO oxidation readily occurs via the tri-molecular Eley-Rideal mechanism, *Phys. Chem. Chem. Phys.* 17 (30) (2015) 20006–20013.
- [68] T. Zhang, Q. Xue, M. Shan, Z. Jiao, X. Zhou, C. Ling, Z. Yan, Adsorption and catalytic activation of O₂ molecule on the surface of Au-doped graphene under an external electric field, *J. Phys. Chem. C* 116 (37) (2012) 19918–19924.
- [69] Z. Gao, W. Yang, X. Ding, G. Lv, W. Yan, Support effects in single atom iron catalysts on adsorption characteristics of toxic gases (NO₂, NH₃, SO₃ and H₂S), *Appl. Surf. Sci.* 436 (2018) 585–595.
- [70] J. Liu, M. Jiao, L. Lu, H.M. Barkholtz, Y. Li, Y. Wang, L. Jiang, Z. Wu, D. Liu, L. Zhuang, C. Ma, J. Zeng, B. Zhang, D. Su, P. Song, W. Xing, W. Xu, Y. Wang, Z. Jiang, G. Sun, High performance platinum single atom electrocatalyst for oxygen reduction reaction, *Nat. Commun.* 8 (2017) 15938.
- [71] A.D. Becke, E.R. Johnson, Exchange-hole dipole moment and the dispersion interaction, *J. Chem. Phys.* 122 (15) (2005) 154104.
- [72] Y. Cheng, S. Zhao, B. Johannessen, J.P. Veder, M. Saunders, M.R. Rowles, M. Cheng, C. Liu, M.F. Chisholm, R. De Marco, H. Cheng, S. Yang, S. Jiang, Atomically dispersed transition metals on carbon nanotubes with ultrahigh loading for selective electrochemical carbon dioxide reduction, *Adv. Mater.* 30 (13) (2018) 1706287.
- [73] H. Yang, S. Hung, S. Liu, K. Yuan, S. Miao, L. Zhang, X. Huang, H. Wang, W. Cai, R. Chen, J. Gao, X. Yang, W. Chen, Y. Huang, H. Chen, C. Li, T. Zhang, B. Liu, Atomically dispersed Ni(i) as the active site for electrochemical CO₂ reduction, *Nat. Energy* 3 (2) (2018) 140–147.
- [74] E. Clementi, D.L. Raimondi, W.P. Reinhardt, Atomic screening constants from SCF functions. II. atoms with 37 to 86 electrons, *J. Chem. Phys.* 47 (4) (1967) 1300–1307.
- [75] X. Sun, P. Han, B. Li, Z. Zhao, Tunable catalytic performance of single Pt atom on doped graphene in direct dehydrogenation of propane by rational doping: a density functional theory study, *J. Phys. Chem. C* 122 (3) (2018) 1570–1576.
- [76] H. Xu, D. Cheng, D. Cao, X. Zeng, A universal principle for a rational design of single-atom electrocatalysts, *Nat. Catal.* 1 (5) (2018) 339–348.
- [77] E. Evans Jr., H. Li, S. Han, G. Henkelman, C. Mullins, Oxidative cross-esterification and related pathways of Co-adsorbed oxygen and ethanol on Pd-Au, *ACS Catal.* 9 (5) (2019) 4516–4525.
- [78] L. Zhao, Y. Zhang, L. Huang, X. Liu, Q. Zhang, C. He, Z. Wu, L. Zhang, J. Wu, W. Yang, L. Gu, H. Lu, L. Wan, Cascade anchoring strategy for general mass production of high-loading single-atomic metal-nitrogen catalysts, *Nat. Commun.* 10 (1) (2019) 1278.
- [79] Q. Luo, W. Zhang, C. Fu, J. Yang, Single Pd atom and Pd dimer embedded graphene catalyzed formic acid dehydrogenation: a first-principles study, *Int. J. Hydrogen Energy* 43 (14) (2018) 6997–7006.
- [80] M.D. Esrafil, P. Nematollahi, R. Nurazar, Pd-embedded graphene: an efficient and highly active catalyst for oxidation of CO, *Superlattice. Microsc.* 92 (2016) 60–67.
- [81] Y. Lee, S. Lee, Y. Hwang, Y.-C. Chung, Modulating magnetic characteristics of Pt embedded graphene by gas adsorption (N₂, O₂, NO₂, SO₂), *Appl. Surf. Sci.* 289 (2014) 445–449.
- [82] X. Guo, S. Huang, Tuning nitrogen reduction reaction activity via controllable Fe magnetic moment: a computational study of single Fe atom supported on defective graphene, *Electrochim. Acta* 284 (2018) 392–399.
- [83] Y. Wang, X. Cui, J. Zhao, G. Jia, L. Gu, Q. Zhang, L. Meng, Z. Shi, L. Zheng, C. Wang, Z. Zhang, W. Zheng, Rational design of Fe-N/C hybrid for enhanced nitrogen reduction electrocatalysis under ambient conditions in aqueous solution, *ACS Catal.* (2018) 336–344.
- [84] J.K. Nørskov, T. Bligaard, A. Logadottir, S. Bahn, L.B. Hansen, M. Bollinger, H. Bengaard, B. Hammer, Z. Sljivancanin, M. Mavrikakis, Y. Xu, S. Dahl, C.J.H. Jacobsen, Universality in heterogeneous catalysis, *J. Catal.* 209 (2) (2002) 275–278.
- [85] H. Li, G. Henkelman, Dehydrogenation selectivity of ethanol on close-packed transition metal surfaces: a computational study of monometallic, Pd/Au, and Rh/Au catalysts, *J. Phys. Chem. C* 121 (49) (2017) 27504–27510.
- [86] J. Rossmeisl, Z. Qu, H. Zhu, G.-J. Kroes, J.K. Nørskov, Electrolysis of water on oxide surfaces, *Electroanal. Chem.* 607 (1–2) (2007) 83–89.

- [87] J. Rossmeisl, A. Logadottir, J.K. Nørskov, Electrolysis of water on (oxidized) metal surfaces, *Chem. Phys.* 319 (1–3) (2005) 178–184.
- [88] Y. Zheng, D. Yang, J.M. Kweun, C. Li, K. Tan, F. Kong, C. Liang, Y.J. Chabal, Y.Y. Kim, M. Cho, J. Yu, K. Cho, Rational design of common transition metal-nitrogen-carbon catalysts for oxygen reduction reaction in fuel cells, *Nano Energy* 30 (2016) 443–449.
- [89] A. Kokalj, P. Gava, S. Degironcoli, S. Baroni, What determines the catalyst's selectivity in the ethylene epoxidation reaction, *J. Catal.* 254 (2) (2008) 304–309.
- [90] S. Linic, J. Jankowiak, M.A. Barteau, Selectivity driven design of bimetallic ethylene epoxidation catalysts from first principles, *J. Catal.* 224 (2) (2004) 489–493.
- [91] J.K. Nørskov, J. Rossmeisl, A. Logadottir, L. Lindqvist, J.R. Kitchin, T. Bligaard, H. Jonsson, Origin of the overpotential for oxygen reduction at a fuel-cell cathode, *J. Phys. Chem. B* 108 (46) (2004) 17886–17892.
- [92] H. Li, L. Luo, P. Kunal, C.S. Bonifacio, Z. Duan, J. Yang, S.M. Humphrey, R.M. Crooks, G. Henkelman, Oxygen reduction reaction on classically immiscible bimetallics: a case study of RhAu, *J. Phys. Chem. C* 122 (5) (2018) 2712–2716.
- [93] B. Corona, M. Howard, L. Zhang, G. Henkelman, Computational screening of core@shell nanoparticles for the hydrogen evolution and oxygen reduction reactions, *J. Phys. Chem.* 145 (24) (2016) 244708.
- [94] F. Li, G. Han, H.-J. Noh, S.-J. Kim, Y. Lu, H.Y. Jeong, Z. Fu, J.-B. Baek, Boosting oxygen reduction catalysis with abundant copper single atom active sites, *Energy Environ. Sci.* 11 (8) (2018) 2263–2269.
- [95] J.K. Nørskov, T. Bligaard, A. Logadottir, J.R. Kitchin, J.G. Chen, S. Pandelov, U. Stimming, Trends in the exchange current for hydrogen evolution, *J. Electrochem. Soc.* 152 (3) (2005) J23–J26.
- [96] B. Zhang, X. Zheng, O. Voznyy, R. Comin, M. Bajdich, M. García-Melchor, L. Han, J. Xu, M. Liu, L. Zheng, F.P. García de Arquer, C.T. Dinh, F. Fan, M. Yuan, E. Yassitepe, N. Chen, T. Regier, P. Liu, Y. Li, P. De Luna, A. Janmohamed, H. Xin, H. Yang, A. Vojvodic, E.H. Sargent, Homogeneously dispersed multimetal oxygen-evolving catalysts, *Science* 352 (6283) (2016) 333–337.
- [97] H. Li, S. Guo, K. Shin, M.S. Wong, G. Henkelman, Design of a Pd-Au nitrite reduction catalyst by identifying and optimizing active ensembles, *ACS Catal.* (2019), <https://doi.org/10.1021/acscatal.9b02182>.
- [98] X. Shen, Y. Pan, B. Liu, J. Yang, J. Zeng, Z. Peng, More accurate depiction of adsorption energy on transition metals using work function as one additional descriptor, *Phys. Chem. Chem. Phys.* 19 (20) (2017) 12628–12632.
- [99] A. Vojvodic, J.K. Nørskov, F. Abild-Pedersen, Electronic structure effects in transition metal surface chemistry, *Top. Catal.* 57 (1–4) (2014) 25–32.